

## Structure of the Squid Axon Membrane as Derived from Charge-Pulse Relaxation Studies in the Presence of Absorbed Lipophilic Ions

Roland Benz\* and Franco Conti

Laboratorio di Cibernetica e Biofisica, Consiglio Nazionale delle Ricerche, 16032 Camogli, Italy

**Summary.** Charge-pulse relaxation studies were performed on squid giant axons in the presence of membrane absorbed lipophilic anions, dipicrylamine (DPA) and tetraphenylborate (TPhB), and of specific blockers of sodium and potassium active currents. With the instrumentation used in this work a time resolution of 5 to 10  $\mu$ sec was easily obtained without any averaging, although the voltage relaxations were always smaller than 5 mV in amplitude in order to keep the membrane voltage in a range where the used theory can be linearized. Two well distinguishable linear relaxations were invariably observed in the presence of the lipophilic anions. With DPA the fast relaxation (time constants between 8 and 70  $\mu$ sec) was attributed to the redistribution of the lipophilic ions within the membrane following the change in membrane potential. The long relaxation process (time constant in the millisecond range) corresponds to the normal voltage relaxation of the passive squid axon membrane slightly modified by the process of redistribution of the extrinsic ions.

The results support the same model for the translocation of lipophilic ions within the nerve membrane proposed earlier for artificial lipid bilayers. The fit of the data with a single barrier model yields the translocation rate constant,  $K$ , and the total concentration,  $N_t$ , of membrane absorbed ions, from which the membrane-solution partition coefficient,  $\beta$ , can be derived. Both for DPA and TPhB,  $K$  had values close to those measured for solvent-free artificial lipid bilayers. The axon membrane appears as fluid mosaic membrane with a thickness of about 2.5 nm for the lipid bilayer part.

In axons treated with DPA the dependence of relaxation data upon the holding membrane potential,  $\bar{E}_m$ , provided information on the asymmetry of

the membrane structure. The data were best fitted by assuming that nearly 100% of the membrane potential drops between the two free energy minima where the extrinsic ions are located, indicating that these minima lie very close to the membrane-solution interfaces, in the region of the phospholipid polar heads. The asymmetry voltage,  $E_o$ , at which the extrinsic ions are expected to be equally distributed between the two sides of the membrane was found to range between  $-35$  and  $-65$  mV (inside negative), depending on the assumed shape of the free energy barrier describing the ion translocation process. This voltage is of the same sign and of the same order of magnitude as the equilibrium voltages for the open-close transitions of the gates of sodium and potassium channels, suggesting that all these voltages result from the same membrane asymmetry. A similar analogy was found between the asymmetry of the free energy barrier which best fitted DPA relaxation data and the asymmetrical voltage dependence of the gating of ionic channels. Our data were best fitted by assuming that about 70% of the potential drop occurs between the free energy minimum on the intracellular membrane face and the top of the barrier.

The structural properties of artificial and biological membranes have been studied in detail in recent years by the use of different probe molecules. Whereas biological membranes have been mostly investigated using fluorescent probes (for reviews *see* Brand & Gohlke, 1972; Weber, 1972; Conti, 1975) or spin-labels (Hubbell & McConnell, 1968), the structure of planar lipid bilayer membranes has been studied to a large extent using charged probes (Anderson & Fuchs, 1975; Szabo, 1976; 1977; Benz & Lauger, 1977; Anderson et al., 1978; Benz & Cros, 1978; Benz & Gisin, 1978; Pickar & Benz, 1978) and only a small

\* Permanent address: Fakultat fur Biologie, Universitat Konstanz, D-7750 Konstanz, West Germany.

number of data is known from optical measurements (Conti & Malerba, 1972; Conti, Fioravanti, Malerba & Wanke, 1974; Webb, 1977). By the incorporation of lipophilic ions, detailed information about dipolar potential (Anderson et al., 1978; Benz & Cros, 1978; Benz & Gisin, 1978; Szabo, 1976; 1977) and membrane thickness (Benz & Lauger, 1977; Pickar & Benz, 1978) could be obtained. In addition, the influence of surface potentials and boundary potentials on ion transport have been investigated (Anderson et al., 1978; Benz & Lauger, 1977; McLaughlin, 1977; McLaughlin & Harary, 1976).

Similar information on the structure and electrical properties of the lipid matrix of biological membranes has been lacking so far due to the difficulty of measuring the kinetics of ionic probes in biological membranes. Nevertheless, the arrangement of the lipid molecules and the dipolar potential probably have a large influence on the function of natural membranes, and these properties cannot be trustworthily inferred from the results of experiments on artificial lipid bilayers. It is still an open question as to what extent the latter experiments have direct biological relevance, a particularly weak point being the necessity of using solvents to form any type of planar lipid bilayer membranes, although from the thermodynamical point of view the role of the solvent may be understood (Benz, Frohlich, Lauger & Montal, 1975; White, Petersen, Simon & Yafuso, 1976).

In nerve membranes the gating of sodium channels, as described by the Hodgkin-Huxley (HH) equations (Hodgkin & Huxley, 1952), is centered around a membrane potential which in squid axons is about  $-35$  mV. Consistently, the charge movements associated with the gating of sodium channels (Armstrong & Bezanilla, 1973; for reviews see Armstrong & Bezanilla, 1975; Almers, 1978; Neumcke, Nonner & Stampfli, 1978) have about the same midpoint potential. The gating of potassium channels as described by the HH equations has also a negative equilibrium potential in the same range (about  $-50$  mV for squid axons). Most likely these potentials arise mainly from local asymmetries experienced by the gating groups because of their attachment to the proteins forming the ionic channels. However, some role of the membrane lipids in establishing these asymmetry potentials cannot be excluded. Electric fields due to asymmetry in the membrane lipids can be monitored by studying the kinetics of ionic probes absorbed in the lipid part of the membrane.

In this work we present measurements of the kinetics of extrinsic ionic probes in the squid axon membrane showing that these ions experience asymmetries similar to those which characterize the voltage dependence of the gating of ionic channels.

These studies may help to understand the role of membrane lipids in the gating mechanism.

The experiments presented in this study were performed using the charge-pulse technique (Feldberg & Kissel, 1975; Benz & Lauger, 1976; Benz, Lauger & Janko, 1976). In this technique the membrane capacitance is charged by a brief current pulse of 50 nsec duration. At the end of the pulse the resistance in the outer circuit is switched to a high value and the voltage across the membrane decays only by charge movements within, and by conductance processes across, the membrane. The charge-pulse method has the advantage of a high time resolution which is provided by the recording system and is not limited by the membrane conductance and capacitance (Benz & Lauger, 1976; Benz, Frohlich & Lauger, 1977). We shall show that this method is also applicable to relaxation studies on squid giant axons where time resolution of 1  $\mu$ sec can be obtained in principle without any averaging. In addition, small voltage signals can be used in the experiments and the perturbation of the membrane can be kept small. We shall show that the kinetics of the translocation of lipophilic ions across the squid axon membrane is fairly accurately described in terms of a simple model. The data suggest that the lipid part of the axon membrane has a thickness of about 2.5 nm, that the intrinsic electric field seen by the ionic probes inside the axon membrane for zero membrane potential has a value similar to that experienced by channel gates, and that there is no obvious formation of lipid domains in the membrane.

## Materials and Methods

### *Axon preparation*

All experiments were performed on giant axons dissected from the hindmost stellar nerve of the squid *Loligo vulgaris*, available in Camogli. The axons were thoroughly cleaned of all surrounding small fibers for a length of 3 to 3.5 cm. They were then placed in a perspex chamber containing a central pool 20 mm in length, separated from the two terminal edges by air gaps of 2 mm width. The central pool was confined by two sliding perspex blocks and could be transformed in a cylindrical space with a cross-sectional diameter of 2 mm. Platinum foils glued to the inner walls of the cylinder and covered with platinum black were used as external current carrying electrodes. They were divided into central (10 mm) and guard ( $2 \times 5$  mm) electrodes according to standard techniques (Moore & Cole, 1963), whenever voltage-clamp responses were monitored. Otherwise they were all connected to ground. The extracellular solution was flown continuously and cooled with a Peltier cooler. The standard artificial seawater (ASW) had the following composition (in mM): 450, NaCl; 10, KCl; 50, CaCl<sub>2</sub>; 1, Tris Cl; pH 7.8. 300 nM Tetrodotoxin (TTX) was added to the ASW in most experiments to abolish sodium currents. Temperature was monitored with a thermistor and kept constant, with a feedback system, within 0.5°C. Most experiments were performed at a temperature of about 12°C.

The axons were perfused intracellularly with the technique of Tasaki, Watanabe and Takenaka (1962), as modified by Rojas and Ehrenstein (1965). The standard perfusion fluid was a  $K^+$ -phosphate solution containing 300 meq  $K^+$  and 350 mM sucrose, pH 7.3. In most experiments 20 mM tetraethylammonium (TEA) chloride was added (substituted for sucrose) to abolish normal potassium currents.

A "piggyback" double electrode assembly (Chandler & Meves, 1965) was introduced in the axon from the end opposite to that from which the perfusion cannula was inserted. Particular care was used in the platinization of the internal current electrode, which was used both to pass current and to monitor the voltage relaxation after charge pulses. The glass pipette of the piggyback assembly, about 80  $\mu\text{m}$  in external diameter, was used to continuously monitor the intracellular DC potential or as normal voltage electrode in standard voltage-clamp measurements. It was filled with 0.5 M KCl, ended with an Ag-AgCl electrode, and contained a floating platinized platinum wire of 20  $\mu\text{m}$  diameter to reduce its resistance. A small polyethylene tubing filled with extracellular solution and with one end close to the axon was used to monitor the extracellular potential with a second Ag-AgCl electrode.

### Electrical Set-up

Figure 1 shows a diagram of the stimulating and recording set-up. The voltage-clamp configuration (with switches 1 and 2 in the solid position) is very simplified and does not show the positive feedback for series resistance compensation (Moore & Cole, 1963), which was present in the actual circuit. The dashed configuration of switches 1 and 2 represents the circuit configuration for charge pulse experiments. Switch 3 represents schematically an electronic switch obtained with FET transistors which could generate pulses as short as 50 nsec. In the open position the effective resistance to ground of the switch was  $10^{12} \Omega$ , and the steady-state membrane potential was set to any desired value by passing through the axon a constant current produced by a variable DC voltage through 1 M $\Omega$  resistor. The relaxation of membrane voltage during a period of less than 1 msec following a charge pulse was monitored directly between the internal and external platinum electrodes. Because of the extremely low impedance of these electrodes at high frequencies, the effective band-width of recording was practically determined only by the input stage of the recording oscilloscope. At the same time the polarization effects which normally prevent the use of platinum electrodes for monitoring signals of longer durations were practically absent in our records of brief voltage relaxations. This was expected because the charge pulse delivered to the axon membrane in our experiments were just enough to raise the membrane potential by at most 5 mV, i.e., a total charge of  $5 \times 10^{-9}$  coulomb/cm<sup>2</sup>. At any rate, the absence of polarization artifacts was checked by applying twice as large pulses to a dummy circuit through the same electrodes, all immersed in artificial seawater. Figure 2 shows such an experiment. In all these cases a purely exponential decay of the voltage with the expected time constant was observed after the charge-pulse.

Records of voltage relaxations were taken with a Polaroid camera from a Tektronix 7633 storage oscilloscope. The shortest relaxation time constant induced by extrinsic hydrophobic ions was of the order of 5  $\mu\text{sec}$ . For this reason most of our recordings were obtained after prefiltering at 1 MHz with a plug-in amplifier (TEK 7A22).

### Analysis of Relaxation Curves

Voltage relaxations following charge pulses were analyzed by assuming that they were composed of two simple exponentials. The time constants and the relative amplitudes of the two components

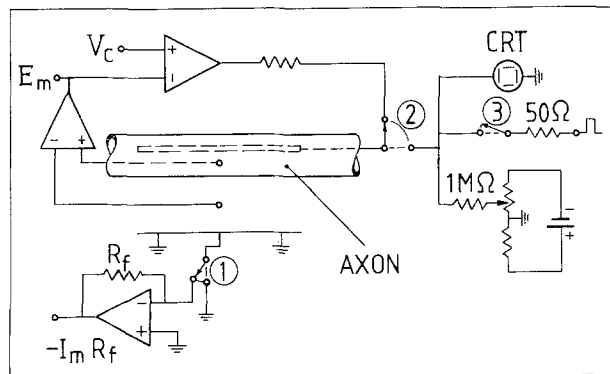


Fig. 1. Schematic diagram of the electrical set-up for charge-pulse and voltage-clamp experiments on squid axon

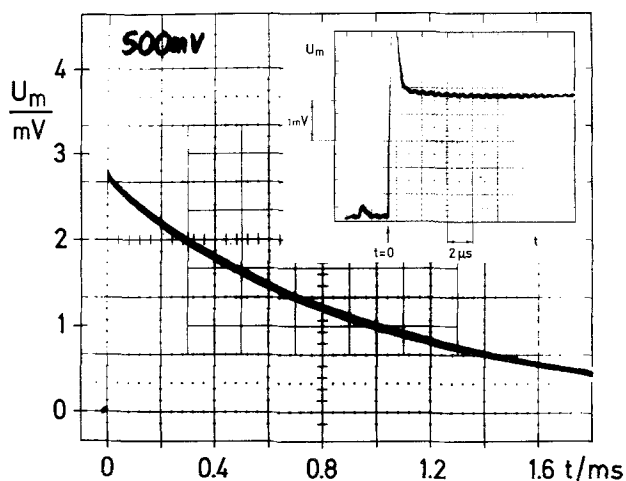


Fig. 2. Oscillographic record of a test experiment with a dummy circuit (300 nF, 3.3 K $\Omega$ ) replacing the membrane in series with the internal and external current electrodes. At  $t=0$  a charge pulse of 50 nsec duration was applied to the whole system. The decay of the voltage is purely exponential with a time constant of about 1 msec and an initial voltage  $U_m(0)$  of about 2.7 mV, which corresponds well with the injected charge of  $8.1 \times 10^{-10}$  A. The inset shows the maximum time resolution which was obtained with this arrangement. The oscillations on the trace were caused by a 1.6 MHz radio station nearby the lab (Radio Camogli)

were determined in two steps after having converted the rough data (Polaroid pictures) in digital form with a digitizer (Summagraphic HV-2-20). Semilogarithmic plots were analyzed first by the simple peel-off method by drawing straight lines through the late part of the record and replotting on a semilogarithmic scale the difference between the original signal and the slow component previously determined (HP-9820 A calculator with 9862 A plotter). In a second step we measured, for each relaxation curve,  $s(t)$ , the time average of  $s(t)$ ,  $ts(t)$ ,  $t^2s(t)$  and  $t^3s(t)$ , and the best fit of  $s(t)$  with the sum of two exponentials was determined according to the least squares deviation of these quantities from their theoretical values (Dyson & Isenberg, 1971). Using as initial values those obtained from the peel-off procedure, the second (iterative) method gave in most cases converging results, considerably improving our estimates. BASIC programs for the above calculations as well as for the fitting of the voltage dependence or relaxation parameters were run on a computer PDP 11/40 (Dig. Eq. Corp. Italia).

## Theory

We develop here the basic equations used to analyze the data presented in this work. The theory is basically identical to that already described in previous papers (Ketterer, Neumcke & Lauger, 1971; Benz et al., 1976), but we have included some generalizations which seem important to interpret our present measurements on nerve membranes. In particular, since most of our measurements were made at membrane potentials different from zero, the dependence of the relaxation parameters on membrane voltage was studied in greater detail.

The model for the transport of lipophilic ions across a membrane postulates that the transport is carried out in three distinct steps: (i) adsorption from the aqueous phase to the membrane-water interface (rate constants  $k'_{am}$  and  $k''_{am}$ ), (ii) translocation of the lipophilic ion between the two energy minima in the membrane (rate constants  $K'$  and  $K''$ ), and (iii) desorption from the membrane to the aqueous phase (rate constants  $k'_{ma}$  and  $k''_{ma}$ ). In the following, it is not a serious restriction to assume that the adsorption-desorption reaction does not play an important role in the experiments described here. This is justified because the exchange of lipophilic ions between membrane and aqueous phase is controlled by slow aqueous diffusion (Benz et al., 1976; Jordan & Stark, 1979) and has time constants in charge-pulse experiments in the order of minutes (Benz et al., 1976), whereas the specific resistance  $R_m$  of the squid axon membrane ( $1 \text{ k}\Omega \text{ cm}^2$ ) predicts relaxation time constants  $\tau_m = R_m \cdot C_m$  ( $C_m$  specific capacitance  $\approx 1 \mu\text{F}/\text{cm}^2$ ) in the order of msec.

The transport of lipophilic ions across the membrane can be described by simple first-order kinetics. Then, the translocation rates  $K'$  and  $K''$  across the barrier from left (intracellular) to right (extracellular) and vice versa have, according to the theory of absolute reaction rates (Johnson, Eyring & Stover, 1974), the following form:

$$\begin{aligned} K' &= (kT/h) \exp\{-\Delta G_1^\ddagger/RT\} \\ K'' &= (kT/h) \exp\{-\Delta G_2^\ddagger/RT\} \end{aligned} \quad (1)$$

where  $k$  is the Boltzmann's constant,  $T$  is the absolute temperature,  $h$  is the Planck's constant,  $R$  is the gas constant, and where the molar free energies of activation,  $\Delta G_1^\ddagger$  and  $\Delta G_2^\ddagger$ , are the differences between the free energy at the top of the barrier and those at the two minima (Fig. 3). The universal frequency  $kT/h$  is about  $6 \times 10^{12} \text{ s}^{-1}$ . The explicit dependence of  $\Delta G_1^\ddagger$  and  $\Delta G_2^\ddagger$  upon the voltage across the membrane,  $E_m$ , and upon the distribution of ions within the membrane is obtained as follows. Let  $x$  be a coordinate

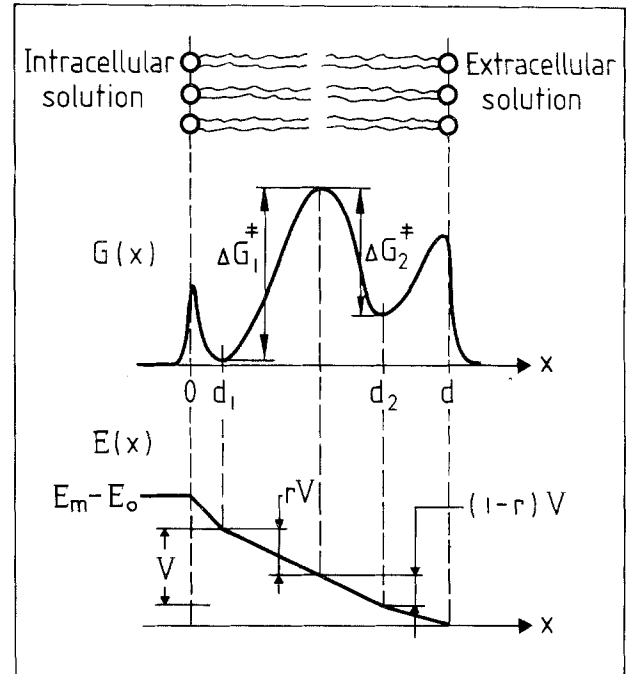


Fig. 3. Schematic diagrams of the free energy profile,  $G(x)$ , and of the relative electric potential profile,  $E(x)$ , seen by lipophilic ions adsorbed near the membrane solution interfaces at the free energy minima  $d_1$  and  $d_2$ .  $E(x)$  is relative to the actual electric potential profile existing for  $E_m = E_o$  and  $\Delta G_1^\ddagger = \Delta G_2^\ddagger$

axis perpendicular to the membrane surface with its origin at the intracellular membrane-solution interface, and let  $d_1$ ,  $d_2$  and  $d$  be the positions of the two minima and the total membrane thickness (see Fig. 3). We can always write:

$$\begin{aligned} \Delta G_1^\ddagger &= \Delta G_o^\ddagger - rzFV \\ \Delta G_2^\ddagger &= \Delta G_o^\ddagger + (1-r)zFV \end{aligned} \quad (2)$$

where:  $\Delta G_o^\ddagger$  is the free energy of activation for ion translocation at the membrane potential,  $E_o$ , for which the ions are equally distributed between  $d_1$  and  $d_2$  in steady-state;  $V$  is the voltage drop between  $d_1$  and  $d_2$ , relative to its steady-state value for  $E_m = E_o$ ;  $r$  is the fraction of  $V$  which drops between  $d_1$  and the top of the barrier;  $z$  is the valence of the ions, and  $F$  is the Faraday's constant. We shall assume that  $r$  is constant, which implies that the membrane is not subject to significant structural changes (e.g., electrostriction) within the range of explored values of  $E_m$ .  $V$  is determined both by  $E_m$  and by the distribution of ions within the membrane. In order to find this dependence, let  $\sigma$  be the surface density of charges in solution at the left interface, in excess of whatever charge distribution is present (for  $E_m = 0$  and in the absence of lipophilic ions) to equilibrate any intrinsic membrane surface charge. Furthermore, let  $N'$  and  $N''$  be the concentrations (in mole/cm<sup>2</sup>) of

ions located at  $d_1$  and  $d_2$ , respectively. The sum of  $N'$  and  $N''$  is considered to be constant during the experiments:

$$N' + N'' = N_t = \text{const} \quad (3)$$

with  $N_t$  total concentration of absorbed lipophilic ions. According to an argument used by Benz et al. (1976) in Eq. (A12) we shall write:

$$E_m = \alpha_1 \sigma / C_m + \alpha_2 (\sigma + zFN') / C_m + \alpha_3 (\sigma + zFN_t) / C_m \quad (4)$$

where  $C_m$  is the membrane capacitance;  $\alpha_1$ ,  $\alpha_2$  and  $\alpha_3$  are structural parameters which correspond to  $d_1/d$ ,  $(d_2 - d_1)/d$ , and  $(d - d_2)/d$  for a membrane with constant dielectric properties. More generally:

$$\alpha_1 + \alpha_2 + \alpha_3 = 1. \quad (5)$$

The second contribution on the right-hand side of Eq. (4) is the actual fraction of  $E_m$  which drops between  $d_1$  and  $d_2$ . Then, according to the definition of  $V$ , we have:

$$V = \alpha_2 \left\{ \sigma + zFN' - \left( \sigma_o + \frac{zFN_t}{2} \right) \right\} / C_m \quad (6)$$

where  $\sigma_o$  is the steady-state value of  $\sigma$  for  $E_m = E_o$  and we have used the notion that for  $E_m = E_o$  the equilibrium value of  $N'$  is  $\frac{N_t}{2}$ .  $\sigma_o$  is obtained from Eq. (4) for

$E_m = E_o$  and for steady-state conditions:

$$E_o = \{ \sigma_o + \alpha_2 zFN_t / 2 + \alpha_3 zFN_t \} / C_m. \quad (7)$$

Equations (4) and (7), taking also into account Eq. (3), can be used to express  $\sigma$  and  $\sigma_o$  in terms of  $E_m$ ,  $E_o$ ,  $N'$  and  $N_t$ . Substituting these expressions into Eq. (6) we obtain:

$$V = \alpha_2 (E_m - E_o) + \alpha_2 (1 - \alpha_2) zF(N' - N_t/2) / C_m. \quad (8)$$

It is convenient for the following treatment to introduce dimensionless parameters and variables:

$$\theta = \frac{z^2 F^2 N_t}{C_m RT} \quad (9)$$

$$\mu = N' / N_t \quad (10)$$

$$u = \frac{zFE_m}{RT}; \quad u_o = \frac{zFE_o}{RT}; \quad v = \frac{zFV}{RT}. \quad (11)$$

$\theta$  is the total charge conferred to the membrane by the lipophilic ions, in units of the amount of charge needed to charge the membrane capacitance to the potential  $\frac{RT}{zF}$ .  $\mu$  is the probability for a lipophilic ion

to be at position  $d_1$ .  $u$ ,  $u_o$  and  $v$  are reduced potentials. The differential equations for  $\frac{du}{dt}$  and  $\frac{d\mu}{dt}$  have the following form (see Appendix):

$$\frac{du}{dt} = \alpha_2 \theta \frac{d\mu}{dt} - \frac{u - \bar{u}}{\tau_m} \quad (12)$$

$$\frac{d\mu}{dt} = -\exp\{r\delta v\} [\bar{K}'\mu - \bar{K}''(1 - \mu)\exp\{-\delta v\}]. \quad (13)$$

This is a system of two differential equations, where the second is nonlinear. The voltage relaxation  $u(t) - \bar{u}$  following a charge-pulse can only be obtained by a numerical solution of Eqs. (12) and (13). However, in the case of small voltage deviations ( $u - \bar{u}$ ) in the charge pulse experiments the differential Eqs. (12) and (13) have the following form (disregarding second or higher order contributions in  $(u - \bar{u})$  or  $(\mu - \bar{\mu})$ ; see Appendix):

$$\frac{du}{dt} = -\alpha_2 \theta \left\{ \bar{K}' + \bar{K}'' + \alpha_2 (1 - \alpha_2) \theta \frac{\bar{K}'\bar{K}''}{\bar{K}' + \bar{K}''} \right\} (\mu - \bar{\mu}) - \left\{ \frac{1}{\tau_m} + \alpha_2^2 \theta \frac{\bar{K}'\bar{K}''}{\bar{K}' + \bar{K}''} \right\} (u - \bar{u}) \quad (14)$$

$$\frac{d\mu}{dt} = - \left\{ \bar{K}' + \bar{K}'' + \frac{\bar{K}'\bar{K}''}{\bar{K}' + \bar{K}''} \alpha_2 (1 - \alpha_2) \theta \right\} (\mu - \bar{\mu}) - \alpha_2 \frac{\bar{K}'\bar{K}''}{\bar{K}' + \bar{K}''} (u - \bar{u}). \quad (15)$$

Equations (14) and (15) are a system of two linear differential equations in the two unknown  $(u - \bar{u})$  and  $(\mu - \bar{\mu})$ . The solution for the voltage relaxation  $u(t) - \bar{u}$  has the following form:

$$u(t) - \bar{u} = a_1 e^{-t/\tau_1} + a_2 e^{-t/\tau_2} \quad (16)$$

or

$$E_m(t) - \bar{E}_m = U_m(t) = U_1 e^{-t/\tau_1} + U_2 e^{-t/\tau_2}. \quad (17)$$

Defining the quantities (see Appendix):

$$Z_1 = \frac{1}{\tau_1} + \frac{1}{\tau_2} \quad (18)$$

$$Z_2 = \frac{1}{\tau_1} \cdot \frac{1}{\tau_2} \quad (19)$$

$$Z_3 = [U_1/\tau_1 + U_2/\tau_2] / (U_1 + U_2) \quad (20)$$

the parameters of the transport are given by:

$$\tau_m = (Z_1 - Z_3) / Z_2 \quad (21)$$

$$2K_{\text{eff}} = \bar{K}' + \bar{K}'' = (Z_1 - Z_3) - \frac{(1 - \alpha_2)}{\alpha_2} \left[ Z_3 - \frac{Z_2}{Z_1 - Z_3} \right] \quad (22)$$

$$\theta = \frac{1}{\alpha_2^2} \frac{\bar{K}' + \bar{K}''}{\bar{K}' \cdot \bar{K}''} \left[ Z_3 - \frac{Z_2}{Z_1 - Z_3} \right]. \quad (23)$$

$K$  and  $N_i$  may be calculated according to:

$$K = \frac{K_{\text{eff}}}{\exp[(r - \frac{1}{2})\bar{v}] \cdot \cosh[\bar{v}/2]} \quad (24)$$

$$N_i = \frac{C_m RT 2 \cosh[\bar{v}/2]}{z^2 F^2 \alpha_2^2 K \cdot \exp[(r - \frac{1}{2})\bar{v}]} \left[ Z_3 - \frac{Z_2}{Z_1 - Z_3} \right] \quad (25)$$

where  $\bar{v}$  is given by Eq. (A25) (see Appendix).

In general, for any fixed value of  $\alpha_2$ ,  $r$  and  $u_o$  Eqs. (22) and (24) yield a value of  $K$  of each charge-pulse experiment at any given value of  $\bar{u}$ . When many measurements for different values of  $\bar{u}$  in the same experimental conditions are available it is possible to look for the values of  $\alpha_2$ ,  $r$  and  $u_o$  which yield the best fit of the experimental data with a constant  $K$ . A similar fit is also possible with Eq. (25). However, because of the large deviation in the data for  $N_i$  (see next section) due to nonstationary adsorption, it was impossible to obtain a proper answer in such a fit.

A critical point of the data analysis is the deviation of Eqs. (14) and (15) because of the first-order approximation. So we have studied the numerical solution of the differential Eqs. (12) and (13) in order to check the validity of the approximation, which allows a simple linearization. The continuous lines in

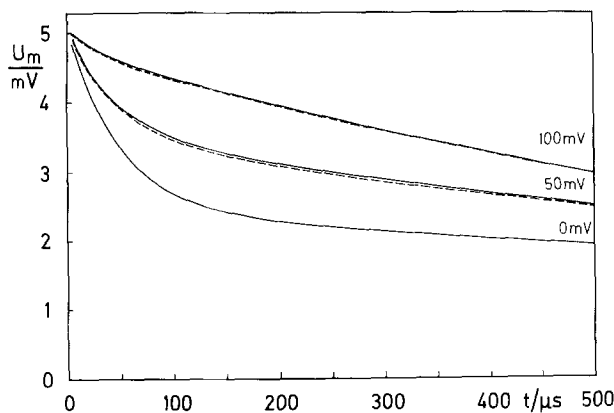


Fig. 4. Comparison between the solution of the differential equations (19) and (21) obtained by first-order approximation (broken lines) and the exact solution (full lines). For the derivation of the curves  $K = 5000 \text{ sec}^{-1}$ ,  $N_i = 10^{-12} \text{ mole cm}^{-2}$  ( $\theta = 4$ ),  $C_m = 1 \mu\text{F cm}^{-2}$ ,  $\tau_m = 1 \text{ msec}$  ( $R_m = 10^3 \Omega \text{ cm}^2$ ),  $u(o) - \bar{u} = 0.2$ , ( $U_m(o) = 5 \text{ mV}$ ) and  $\bar{u} - u_o = 0$  ( $\bar{E}_m - E_o = 0 \text{ mV}$ ),  $\bar{u} - u_o = 2$  ( $\bar{E}_m - E_o = 50 \text{ mV}$ ) and  $\bar{u} - u_o = 4$  ( $\bar{E}_m - E_o = 100 \text{ mV}$ ) were used. For  $E_m - E_o = 0$  the exact solution and the first-order approximation show superposition

Fig. 4 show the time course of  $u(t) - \bar{u}$  obtained from numerical solutions of Eqs. (12) and (13) and for the following values of the parameters, which have been found to be adequate to describe the relaxation of the membrane potential in the presence of DPA (see next section):

$$K = 5 \times 10^3 \text{ s}^{-1}; \quad \alpha_2 = 1; \quad r = 0.5; \quad \theta = 4$$

(i.e.,  $N_i = 10^{-12} \text{ mole/cm}^2$ ;  $C_m = 1 \mu\text{F/cm}^2$ );  
 $\tau_m = 10^{-3} \text{ sec}$ ; and for  $\bar{u} - u_o = 0$ ,  $\bar{u} - u_o = 2$ ;  
and  $\bar{u} - u_o = 4$ .

The dashed lines in Fig. 4 were obtained from the solution of Eqs. (14) and (15) using the same parameters. As can be seen from Fig. 4 the difference between the exact solution and the first-order approximation is rather small, and it is not possible to distinguish between the different solutions in the limit of the experimental errors.

## Results

### Kinetics of the DPA Transport

If the membrane of a squid giant axon, in the presence of TTX and TEA but no extrinsic ionic probes, is charged by a brief current pulse of 50 nsec duration to an initial voltage between 5 and 10 mV, the voltage across the membrane decays in three relaxation processes to the holding potential,  $E_m$ . The fastest relaxation process has a time constant in the range of 1 to 2  $\mu\text{sec}$  and an amplitude of 40–50% of the total relaxation amplitude. This relaxation process is presumably related to particular structural properties of the squid giant axon preparation and reflects a non-uniform accessibility of the axolemma through the resistance of the Schwann cell layer (R. Benz and F. Conti, unpublished results). This component will not be considered in further detail in this study. The second relaxation process has a time constant in the range of 100 to 200  $\mu\text{sec}$  and contributes to about 5% of the total amplitude. It is likely that this relaxation is due to the movement of gating particles within the membrane (R. Benz and F. Conti, unpublished results). Neither will this process be analyzed further in this work. Although the time constant of this relaxation is of the same order of magnitude of that of the fast relaxation produced by DPA and TPhB, we always worked at such high concentrations of DPA and TPhB that its amplitude was negligible with respect to the relaxation of the lipophilic ions.

The third (longest) relaxation reflects the time constant,  $\tau_m = R_m C_m$ , of the membrane. It was found to be of the order of milliseconds, corresponding to a specific resistance of the squid axon membrane of at

least  $10^3 \Omega \text{cm}^2$ , assuming  $C_m \sim 1 \mu\text{F} \cdot \text{cm}^{-2}$ .  $R_m$  was found to be dependent on the holding potential,  $\bar{E}_m$ . For depolarizing voltages ( $\bar{E}_m > -50 \text{ mV}$ )  $R_m$  tended to decrease, probably because of incomplete block of  $\text{K}^+$  channels by TEA.

One of the charge-pulse experiments with an unmodified squid axon is shown in Fig. 5. The axon membrane is charged by a brief current pulse of 50 nsec duration to a voltage of about 5 mV. The decay of the voltage with time is recorded with three different sweep times: 20, 100, and 500  $\mu\text{sec}/\text{div}$ . The figure shows oscillographic records directly photographed with a Polaroid camera. It is seen that the time resolution of the charge-pulse experiments on squid giant axons is very good. The records of Fig. 5 were taken with 1 MHz bandwidth. However, it is possible to obtain similar records with a higher bandwidth (e.g., 5 MHz), easily reaching time resolutions close to 500 nsec (R. Benz and F. Conti, *unpublished results*). This is about 20 times better a resolution than in voltage-clamp experiments and constitutes the major advantage of the charge-pulse relaxation method.

In preliminary experiments with DPA we first tried to apply DPA only extracellularly. However, even after waiting for periods of the order of 1 hr after the application of the lipophilic ions, we could detect very little changes in the electrical properties of the squid axon membrane in those conditions. This observation is qualitatively consistent with the notion that the absorption of lipophilic ions by the membrane is rate limited extracellularly by the presence of the Schwann layer (Frankenhauser & Hodgkin, 1956), as already discussed at the beginning of the previous section. When lipophilic ions are applied only from the extracellular side, the absorption process is further slowed down because desorption from the intracellular membrane face into the axoplasm is faster than the absorption process on the opposite face. The concentration of absorbed ions remains then very small as long as the axoplasmic concentration is low. Therefore we decided to use routinely squid axons perfused both intracellularly and extracellularly with the same concentration of DPA. Although this procedure considerably speeded up the time required to see effects of the desired size, still long times were occasionally needed in order to obtain steady-state conditions in the response of the axon membrane to the action of DPA. The reason for this variability of the axons' behavior is presumably caused by the more or less extensive removal of axoplasm in different preparations. The data presented here were all obtained from axons which were exposed to the lipophilic ions for a time of the order of 1 hr.

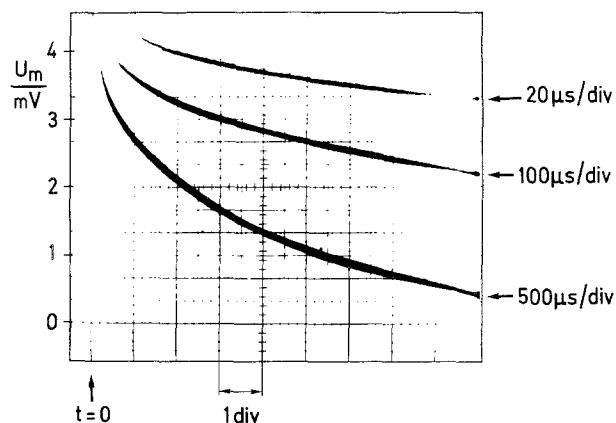


Fig. 5. Decay of the membrane voltage  $U_m$  after a charge pulse of 50 nsec duration applied to an unmodified squid axon. The decay of  $U_m$  was recorded with different sweep times as indicated on the right side of the oscillogram.  $T=13^\circ\text{C}$ ;  $U_m(o) \sim 6 \text{ mV}$ ;  $\bar{E} = -40 \text{ mV}$

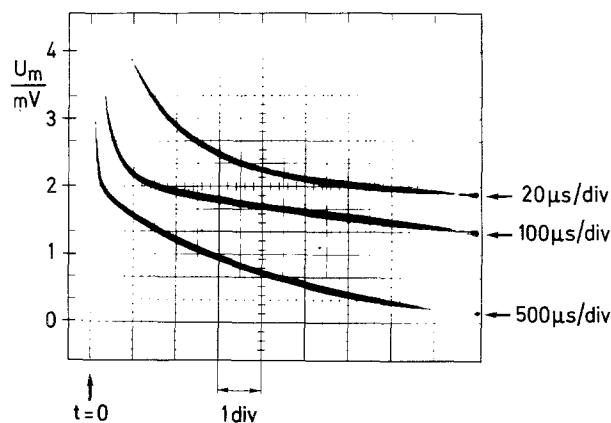


Fig. 6. Decay of the membrane voltage  $U_m$  after a charge pulse of 50 nsec duration applied to the same axon of Fig. 5 in the presence of  $10^{-7} \text{ M}$  dipicrylamine (internally and externally for 60 min). The decay of  $U_m$  was recorded with different sweep times as indicated on the right side of the oscillogram. The data were fitted according to Eq. (16) with the following parameters:  $\tau_1 = 3.1 \times 10^{-3} \text{ sec}$ ,  $a_1 = 0.137$ ,  $\tau_2 = 2.02 \times 10^{-3} \text{ sec}$ ,  $a_2 = 0.086$ ,  $U_m(o) = 5.51 \text{ mV}$ ,  $T = 13^\circ\text{C}$ ,  $\bar{E}_m = -40 \text{ mV}$ .  $K = 6.4 \times 10^3 \text{ sec}^{-1}$  and  $N_i = 1.6 \times 10^{-12} \text{ mole cm}^{-2}$  were calculated according to Eqs. (18)–(25) using  $\alpha_2 = 1$ ,  $r = 0.5$ ,  $\bar{v} \sim 0$ , and  $C_m = 1 \mu\text{F cm}^{-2}$ ;  $\beta = 1.6 \times 10^{-2} \text{ cm}$

All the experiments reported in what follows were performed on axons treated with large concentrations of TTX and TEA, in order to remove any relaxation process associated with the normal development of the ionic currents responsible for membrane excitability. However, the possible influence of the lipophilic ions on the normal excitability of squid axons was also studied in preliminary experiments. These showed that the voltage-clamp currents were not significantly affected by the presence of lipophilic ions added in the bathing media at concentrations below  $10^{-6} \text{ M}$ . Higher concentrations of lipophilic

ions significantly modified the voltage-clamp characteristics of the axons without abolishing excitation. For example,  $10^{-5}$  M-TPhB produced a general shift of about 20 to 30 mV (in the depolarizing direction) in the voltage dependence of the axon responses.

Figure 6 shows a charge-pulse experiment taken from the same axon as in Fig. 5 after the addition in the bathing solutions of  $10^{-7}$  M DPA. The figure shows clearly that the presence of  $10^{-7}$  M DPA produces a much stronger decay of the voltage across the membrane at short times. Such decay is caused by the fast displacement of the lipophilic ions. The fast decay of the membrane voltage is even more pronounced at higher concentrations of the lipophilic ions as seen in Fig. 7 for an experiment with  $3 \times 10^{-7}$  M DPA. Figure 7 shows an evident increase of the amplitude of the fast relaxation process, whereas the amplitude of the slow relaxation decreases.

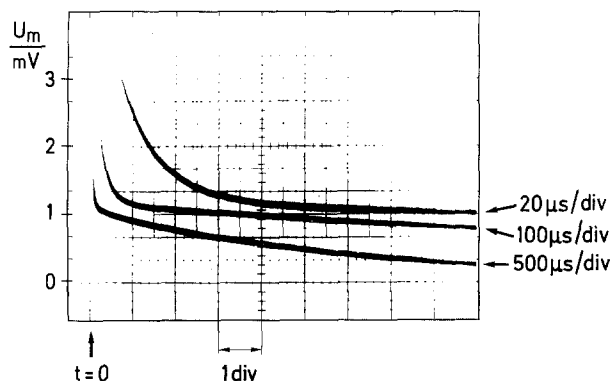


Fig. 7. Decay of the membrane voltage  $U_m$  after a charge pulse of 50 nsec duration applied to the same axon of Fig. 5 in the presence of  $3 \times 10^{-7}$  M dipicrylamine (internally and externally for 60 min). The decay of  $U_m$  was recorded with different sweep times as indicated on the right side of the oscillogram.  $T=13^\circ\text{C}$ ;  $\bar{E}_m = -40$  mV.

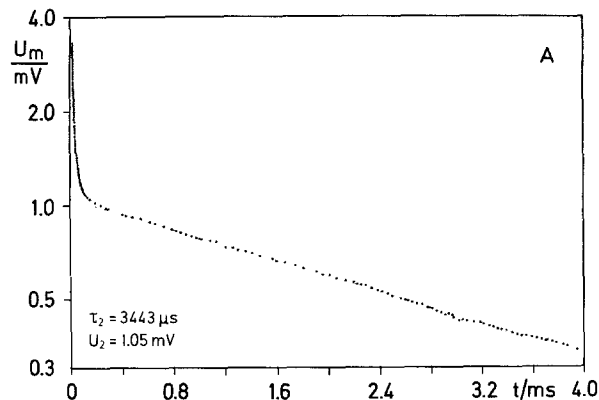


Figure 8 shows a semilogarithmic plot of the data presented in Fig. 7. It is evident from this figure that the decay of the membrane voltage after a charge pulse can be well described by a sum of two exponentials as required by the description of the transport model.

The voltage dependence of the DPA transport was measured in six different axons for eight independent conditions. For any particular condition (determined by the particular axon and by the concentration of DPA in solution) a minimum of six charge-pulse relaxation measurements at different membrane potentials was performed. The membrane voltage relaxation could be fitted in each case with two exponentials according to the presented theory. From the time constants and the relative amplitudes of these relaxations,  $N_i$  and  $K_{\text{eff}}$  were calculated for any assumed value of  $\alpha_2$  according to Eqs. (18)–(25). Figure 9 shows a plot of  $K_{\text{eff}}$  versus membrane potential for one of these experiments and assuming  $\alpha_2 = 1$ . It is seen that  $K_{\text{eff}}$  is clearly changing with  $\bar{E}_m$ , showing a minimum in the range between  $-60$  and  $-10$  mV. The curves through the data were obtained by best fitting the data according to Eq. (24) for  $r = 0.5$  and for  $r = 0.73$ , respectively. Both curves seem to yield a fair fit of the data, although a quantitative inspection would show that the curve for  $r = 0.73$  gives a substantially better fit. In general, each set of  $K_{\text{eff}}$  data calculated from Eq. (22) for any particular value of  $\alpha_2$ , was best fitted according to Eq. (24) for various values of  $r$ . The error of the fit, as measured by the relative rms deviation of  $K_{\text{eff}}$  from its theoretical value, depended strongly upon  $\alpha_2$  but showed a relatively shallow minimum as a function of  $r$ , for any fixed value of  $\alpha_2$ . Thus, the fit error was almost doubled when  $\alpha_2$  was decreased from 1 to 0.94, for a constant  $r$ , while the sharpest dependence of the fit

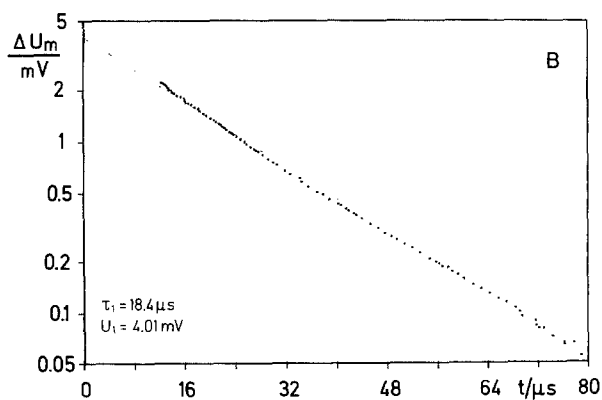
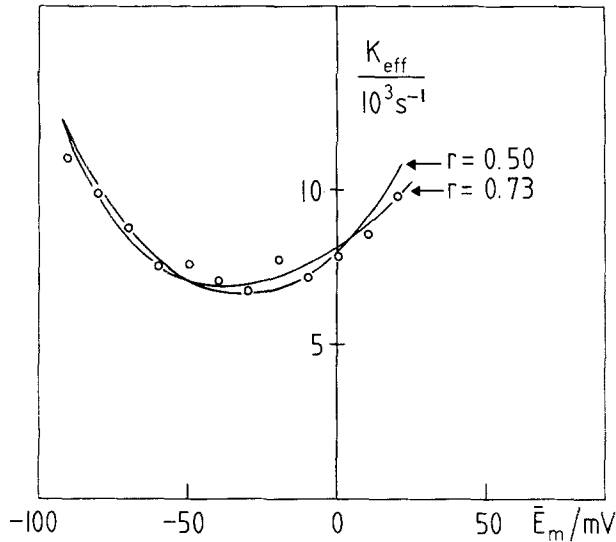


Fig. 8. Analysis of the data of Fig. 7. The relaxation times  $\tau_i$  and the voltage amplitudes  $U_i$  [Eq. (17)] were evaluated by the two successive plots A and B. In each case the regression line was drawn which gave the best fit to the plotted points. From the data given in A and B the following values for  $K$ ,  $N_i$  and  $\beta$  were calculated ( $C_m = 1 \mu\text{F cm}^{-2}$ ,  $\alpha_2 = 1$ ,  $r = 0.5$ ,  $\bar{v} \sim 0$ ):  $K = 5.8 \times 10^3 \text{ sec}^{-1}$ ,  $N_i = 3.8 \times 10^{-12} \text{ mole/cm}^2$  and  $\beta = 1.3 \times 10^{-2} \text{ cm}$



error upon  $r$ , obtained for  $\alpha_2=1$ , was an increase from 4.9 to 6.1% when  $r$  decreased from 0.73 to 0.5. Any value of  $\alpha_2$  greater than unity is physically unacceptable since the model requires  $\alpha_2 \leq 1$ . It was



**Fig. 9.**  $K_{\text{eff}}$  as a function of the membrane potential  $\bar{E}_m$  as derived from charge-pulse relaxation studies with a squid axon (experiment 3-1;  $3 \times 10^{-7}$  M DPA,  $T=13^\circ\text{C}$ ) assuming  $\alpha_2=1$  [Eqs. (27), (29), (33) and (38)]. The curves were drawn according to Eqs. (34) and (39) using the indicated values for  $r$

interesting, however, to observe that indeed the fit became very rapidly worse when  $\alpha_2$  exceeded unity, in good support of the model. From this type of analysis, we found that our data on DPA kinetics were best described by the model of Fig. 3 assuming  $\alpha_2=1$  and  $r=0.73$ . Table 1 gives the values of  $K$  and  $E_o$  obtained from the best fit of eight different set of data of the type shown in Fig. 9 (obtained for  $\alpha_2=1$ ) for  $r=0.73$  and  $r=0.5$ . The table also gives the values of the fit errors showing that for  $r=0.5$  a worse overall fit is obtained, although the fit is better in several experiments. For this reason we cannot stress too much the suggestion derived from our present data that  $r$  might actually be as large as 0.73. As can be seen from the data of Table 1, there is a relatively small scatter in the data for  $K$  independent of the chosen value for  $r$  and we believe that such scatter might reflect differences between various preparations more than experimental errors, as suggested by the closer agreement between  $K$  values obtained from different experiments on the same preparation (expts. 3-1 and 3-2 and expts. 6-1 and 6-2). The table also shows that for any fixed value of  $r$  the scatter of  $E_o$  values obtained for the individual runs was of the order of  $\pm 5$  mV, which is rather small, considering the shallowness of the voltage dependence of  $K_{\text{eff}}$ .

**Table 1.** Kinetic data of DPA transport across squid axon membrane<sup>a</sup>

Exp.	$n$	$c_{\text{DPA}}/\text{M}$	$K/10^3 \text{ sec}^{-1}$	$E_o/\text{mV}$	$N_i/\text{pmol cm}^{-2}$	$\beta/10^{-3} \text{ cm}$	$\sqrt{\left\langle \left( \frac{\Delta K_{\text{eff}}}{K_{\text{eff}}} \right)^2 \right\rangle}$
A) Fit with $\alpha_2=1$ ; $r=0.73$ (see text)							
1	6	$10^{-6}$	6.81	-56.5	1.8	0.9	0.033
2	9	$10^{-6}$	6.90	-66	2.4	1.2	0.048
3-1	12	$3 \times 10^{-7}$	7.71	-61.5	2	3.3	0.046
3-2	7	$10^{-6}$	7.31	-69.5	5.6	2.8	0.016
4	9	$3 \times 10^{-8}$	5.08	-63	1.5	25	0.054
5	9	$10^{-7}$	5.08	-71.5	0.6	3	0.039
6-1	12	$3 \times 10^{-7}$	8.33	-68	1.2	2	0.066
6-2	12	$3 \times 10^{-6}$	9.09	-59.5	3.4	0.57	0.055
Mean value			7.04	-64.5			0.049
$\pm$ SD			$\pm 1.42$	$\pm 5$			
B) Fit with $\alpha_2=1$ ; $r=0.5$ (see text)							
1	6	$10^{-6}$	5.8	-25	2.1	1.1	0.077
2	9	$10^{-6}$	6.03	-38.1	3.1	1.6	0.030
3-1	12	$3 \times 10^{-7}$	6.63	-31.5	2.5	4.1	0.062
3-2	7	$10^{-6}$	6.47	-44.5	6.8	3.4	0.014
4	9	$3 \times 10^{-8}$	4.45	-36.5	1.7	28	0.037
5	9	$10^{-7}$	4.43	-40.0	0.6	3	0.063
6-1	12	$3 \times 10^{-7}$	7.09	-34.5	1.3	2.2	0.107
6-2	12	$3 \times 10^{-6}$	7.84	-30.5	4.2	0.7	0.026
Mean value			6.09	-35.0			0.061
$\pm$ SD			$\pm 1.20$	$\pm 6$			

<sup>a</sup>  $n$  is the number of different voltages  $\bar{E}_m$  used in one set of experimental conditions;  $T=13^\circ\text{C}$ .

According to Eqs. (23) and (25) the concentration of absorbed lipophilic ions,  $N_t$ , can also be determined from the same data used to determine  $K$  and  $E_o$ . In principle, if we assume that  $N_t$  is voltage independent, Eq. (25) could be used to obtain the best guess of  $\alpha_2$  and  $E_o$ , leading to the least squares deviation of  $\theta$  from a constant value. For consistency these guesses should agree with those obtained from the fitting of  $K_{\text{eff}}$  data according to Eq. (24) as previously described. In performing such analysis we found that Eq. (23) could not be satisfied with a constant  $\theta$  with any accuracy comparable with that obtained in the fit of  $K_{\text{eff}}$  data. The smallest scattering of  $\theta$  values which could be obtained within any given experiment was in most cases of the order of 20%. Furthermore, such least squares fit was obtained for  $\alpha_2$  close to 0.9, a value which was far too low for a good fit of  $K_{\text{eff}}$  data. On the other hand, the value of  $N_t$  calculated from Eqs. (23) and (25) using the values of  $\alpha_2$  and  $E_o$  which best fitted  $K_{\text{eff}}$  data showed a strong dependence on membrane potential. We believe that this fact does not invalidate the theoretical model but it implies that the assumption that  $N_t$  is constant is not valid. One reason for  $N_t$  variations may be related to the difficulty of establishing partition equilibria for DPA between the aqueous phases and the membrane, most in the same way as it has been found for experiments with lipid bilayer membranes (Benz et al., 1976; Wulf, Benz & Pohl, 1977). Indeed, from Table 1 it is seen that there is a large scatter of  $N_t$  values obtained from different experiments with the same DPA concentration. The values of  $N_t$  reported in Table 1 were obtained from Eq. (25) for  $\bar{u}=u_o$  and assuming  $C_m = 1 \mu\text{F}/\text{cm}^2$ . From these values the apparent partition coefficient,  $\beta = N_t/2c$ , was calculated and this quantity is also reported in Table 1. It is clear that  $\beta$  tends to decrease for increasing DPA concentrations. This might imply that we have used in most of our experiments DPA concentrations for which the absorption of DPA by the membrane is near saturation. Indeed, the lowest DPA concentration used,  $3 \times 10^{-8} \text{ M}$ , yielded an extremely high partition coefficient, about 40 times larger than the one measured for  $C_{\text{DPA}} = 3 \times 10^{-6} \text{ M}$ .

In experiments with squid axon no clear influence of DPA concentration upon the values for  $K$  was observed. However, the concentration dependence of  $\beta$  (Table 1) provides quite good evidence for boundary-potential effects (McLaughlin, 1977).

In two different axons the temperature dependence of the DPA kinetics was measured. Increasing the temperature from 12 to 23°C,  $K$  increased from  $6 \times 10^3 \text{ sec}^{-1}$  to  $10^4 \text{ sec}^{-1}$ , i.e., by a factor of 1.7, which corresponds to an activation energy of about 33 kJ/

mol (8 kcal/mol). This activation energy compares very well to the activation energies measured in lipid bilayer membranes for the translocation rate constant of DPA (Benz et al., 1976). The total concentration of DPA decreased a little between 13 and 23°C. This finding is consistent with the observation in lipid bilayer membranes that the adsorption of lipophilic ions is partly entropy driven (Bruner, 1975; Benz et al., 1976). However, the above-discussed possible drifts of  $N_t$  during the experiments do not allow us to give a reliable estimate of the activation energy of  $N_t$ .

### Kinetics of Tetraphenylborate Transport

The kinetics of TPhB transport in the squid axon membrane was not studied as extensively as that of DPA. In two experiments on different axons charge pulse relaxations were measured for  $C_{\text{TPhB}} = 3 \times 10^{-7} \text{ M}$  and for  $\bar{E}_m$  around  $-30 \text{ mV}$ . Two major relaxation processes were found as in the case of axons treated with DPA. The same type of analysis described in the previous section yielded the following average values for  $K$ ,  $N_t$  and  $\beta$ , assuming  $C_m = 1 \mu\text{F}/\text{cm}^2$ ,  $\alpha_2 = 1$ , and  $E_o \sim \bar{E}_m$ :

$$K = 450 \pm 50 \text{ sec}^{-1}, \quad N_t = 3(\pm 1) \times 10^{-13} \text{ mol}/\text{cm}^2, \\ \beta = 0.5 \times 10^{-3} \text{ cm}.$$

The value of the translocation rate constant  $K$  for TPhB transport is about 15 times smaller than the corresponding value for DPA. The corresponding value for the ratio  $K_{\text{DPA}}/K_{\text{TPhB}}$  in lipid bilayer membranes is only slightly higher, between 20 and 40 (Anderson & Fuchs, 1975; Benz et al., 1976), and it is not clear if this difference should be taken as indicative of major structural differences between the two preparations.

### Discussion

The results presented in this paper show that the same model developed for the transport of lipophilic ions in artificial lipid bilayer membranes is also adequate to describe the transport of these ions across the squid axon membrane. This suggests that the nerve membrane contains large domains where the lipid is arranged as a lipid bilayer, a statement which supports the fluid mosaic model of Singer and Nicholson (1972).

The kinetics of DPA or TPhB in the squid axon membrane appears to be much faster than in artificial lipid bilayers containing solvents (Benz & Läuger, 1977; Pickar & Benz, 1978). Taking into account also temperature effects the translocation rate constants in the nerve membrane are about 40 times larger than

in solvent containing artificial bilayers and are also larger than, but comparable to, those measured in solvent-free membranes (Benz & Läuger, 1977). This finding may have several reasons. One reason may be that the content of phosphatidylethanolamine in the squid axon membrane tends to hasten the kinetics of lipophilic ions as it does in artificial lipid membranes (Benz & Läuger, 1977). Another possibility is that the dielectric constant of the squid axon membrane may be increased because of the presence of proteins. This would result in a lower free-energy barrier and therefore in faster kinetics of the ionic probes (Dilger, McLaughlin, McIntosh & Simon, 1980), as well as in higher values of the specific capacitance (as found by Dilger et al., 1980). Finally, the higher value of the capacity as well as the faster kinetics could also be the consequence of a smaller membrane thickness. In black films a strong correlation between the kinetics of DPA or TPhB translocation and membrane thickness is observed (Benz & Läuger, 1977; Pickar & Benz, 1978), which can be very well described by the image force model (Neumcke & Läuger, 1969; Parsegian, 1969). According to measurements of membrane capacitance, solvent-free lipid bilayer membranes have a hydrocarbon thickness of about 2.5 nm. If we interpret our results considering only this effect, our data would imply that the thickness of the hydrocarbon layer in the squid axon membrane is of the order of 2.0–2.5 nm. This would correspond to a total membrane thickness, including the polar layers, of 3 to 3.5 nm.

The voltage dependence of DPA kinetics, analyzed in this work, was found to be consistent with a value of the parameter  $\alpha_2$  close to unity. The same result was obtained in lipid bilayers, and it implies that the free energy minima where the lipophilic ions are located lie just at the membrane-solution interfaces, probably in the phospholipids' polar head regions, as expected for typically amphipatic molecules as DPA.

The other parameter which could be evaluated from the analysis of the voltage dependence of DPA transport in the squid axon membrane was the asymmetry voltage,  $E_o$ . Within any reasonable allowance for experimental errors,  $E_o$  was found to range between  $-35$  and  $-65$  mV, quite different from that expected for a symmetric membrane and found in symmetric artificial bilayers. It is unavoidable to compare this property of lipophilic ion translocation with the voltage dependence of ionic channel gates, as described by the HH equations, which have equilibrium potentials of about  $-35$  and  $-50$  mV for sodium and potassium channels, respectively. The asymmetric displacement currents believed to be associated with the movements of the charged groups

responsible for the gating of sodium channels (Armstrong & Bezanilla, 1973; see recent reviews by Armstrong & Bezanilla, 1975; Almers, 1978; Neumcke, Nonner & Stämpfli, 1978) have midpoint potentials in qualitative agreement with the HH model. Our finding that the asymmetry voltage seen by extrinsic lipophilic ions is of the same sign and numerically close to that seen by the gating structures of ionic channels might suggest a common origin of such voltages. A substantial similarity between the properties of extrinsic ions and gating groups, could indeed exist if the latter structures were groups bearing a net charge and moving rather freely at the periphery of the ionic channels. One should be aware, however, that the above similarities might very well be fortuitous. The voltage sensing groups which gate ionic channels are likely to have free-energy profiles determined to a major extent by their tight binding to membrane proteins and/or by their dipolar character. Indeed, it is worth noticing here that in the frog node the asymmetry voltage, as derived from gating current measurements, has very different values for DPA<sup>-</sup> and for the gating of Na<sup>+</sup>-channels (Benz & Nonner, 1980). In this case  $E_o$  for DPA<sup>-</sup> ranges between 0 and 30 mV, whereas  $E_o$  for the gating charge movement ranges between  $-20$  and  $-40$  mV.

The question of compartmentation of the lipids in biological membranes has been discussed in detail in recent years (for a review see Sackmann, 1978). Some data have been presented pointing to the existence of lipid domains and of some sort of annulus around membrane proteins having a lipid composition quite different from that of the bulk lipid phase (Sackmann, 1978). These results have been questioned by recent NMR studies, where no evidence for compartmentation down to 1  $\mu$ sec time resolution has been found (Seelig & Seelig, 1978). According to these studies the exchange of lipids between different compartments, assuming that such compartments exist, occurs in much less than 1  $\mu$ sec. In agreement with this we found no indication, within our time resolution of about 5  $\mu$ sec, that the fast component of our voltage relaxation could be further split into two or more components, possibly associated with the movement of lipophilic ions within domains of different lipidic composition. Thus, we found no evidence for a domain structure in the lipidic part of squid axon membrane. However, we cannot stress this point too much because we could only detect the presence of a compartmentation if the time constants of the DPA or TPhB relaxation differed in the various domains by at least a factor of two. Furthermore, if the compartmentation is only limited to lipids either free or adsorbed on proteins, then it could be that the

latter constitute only a minor part of the total lipids and their effect on the average properties of the whole membrane would be hardly seen.

From the results presented here we conclude that there is a strong analogy between artificial lipid bilayer membranes and the lipid bilayer part of a nerve membrane and that the movement of charged particles across both types of membranes is adequately described by the same simple model involving a simple free energy barrier. This finding contradicts the results which have been found by Conrad and Singer (1979) for the partitioning of amphipatic compounds in biological membranes and lipid vesicles. In these experiments the partition coefficients for chlorpromazine, 2,4 dinitrophenol and 1-decanol have been found to be at least by 1000 times smaller in the biological membrane than in lipid vesicles, a result not supported by the data obtained in this study.

The present study was limited to the interaction of extrinsic ionic probes with the nerve membrane. However, we believe that in the near future the charge pulse relaxation method will also offer the possibility of gaining new insight into the properties of intrinsic ionic groups in the squid axon membrane, such as those governing the gating of ionic channels.

The authors wish to thank Dr. P. Lauger for many helpful discussions. The excellent technical assistance of Mr. G. Boido, Mr. G. Ehmann, and Miss F. Lenssen has been of invaluable help throughout the experimental work and the reduction of the data.

This work has financially been supported by the Deutsche Forschungsgemeinschaft (Sonderforschungsbereich 138). The support by two EMBO short term fellowships to one of us (R.B.) is gratefully acknowledged.

## Appendix

Derivation of Eqs. (12)–(15) and (18)–(25): With the definitions (9)–(11), Eq. (8) becomes:

$$v = \alpha_2(u - u_0) + \alpha_2(1 - \alpha_2)\theta(\mu - \frac{1}{2}). \quad (\text{A1})$$

Equation (A1) allows us to write explicitly the general dependence of the rate constants  $K'$  and  $K''$  upon lipophilic ion distribution and membrane potential. From Eqs. (1), (2), (11) and (A1) the rate constants  $K'$  and  $K''$  during a relaxation experiment can then be expressed as:

$$K' = \bar{K}' \exp\{r\delta v\} = K \exp\{r\bar{v}\} \exp\{r\delta v\} \quad (\text{A2})$$

$$K'' = \bar{K}'' \exp\{(r-1)\delta v\} = K \exp\{(r-1)\bar{v}\} \exp\{(r-1)\delta v\} \quad (\text{A3})$$

where, from here on, the bar denotes the steady-state value of any quantity,  $K$  is the equilibrium rate constant for ion translocation at  $E_m = E_0$ :

$$K = \frac{\kappa T}{h} \exp\{-\Delta G_o^\ddagger / RT\} \quad (\text{A4})$$

and where  $\bar{v}$  and  $\delta v$  are given by:

$$\bar{v} = \alpha_2(\bar{u} - u_0) + \alpha_2(1 - \alpha_2)\theta(\bar{\mu} - \frac{1}{2}) \quad (\text{A5})$$

$$\delta v = \alpha_2(u - \bar{u}) + \alpha_2(1 - \alpha_2)\theta(\mu - \bar{\mu}). \quad (\text{A6})$$

The differential equations for the time course of  $u(t)$  and  $\mu(t)$  during a charge pulse relaxation experiment are obtained from the definition of  $K'$  and  $K''$ :

$$\frac{d\mu}{dt} = -K'\mu + K''(1 - \mu) \quad (\text{A7})$$

and from the equation of continuity of the electric current:

$$\frac{\bar{E}_m}{R_m} = \frac{E_m}{R_m} + \frac{d\sigma}{dt} \quad (\text{A8})$$

where  $R_m$  is the membrane resistance per unit surface and  $\bar{E}_m/R_m$  is the constant current density provided by the current generator to maintain across the membrane the steady-state potential,  $\bar{E}_m$ . By taking the time derivative of the expression of  $\sigma$  in terms of  $E_m$  and  $N'$ , as it can be obtained from Eq. (4), and substituting it into Eq. (A8) we obtain:

$$\frac{du}{dt} = \alpha_2\theta \left\{ \frac{d\mu}{dt} - \frac{u - \bar{u}}{\tau_m} \right\}. \quad (\text{A9})$$

Substituting for  $K'$  and  $K''$  the expressions given in Eqs. (A2) and (A3), Eq. (A7) becomes:

$$\frac{d\mu}{dt} = -\exp\{r\delta v\} \{ \bar{K}'\mu - \bar{K}''(1 - \mu) \exp\{-\delta v\} \}. \quad (\text{A10})$$

Together with Eq. (A6), Eqs. (A9) and (A10) constitute a system of two differential equations where Eq. (A10) is nonlinear. The linear approximation is obtained considering that in our experiments ( $u - \bar{u}$ ), and consequently also  $\delta v$  (see Eq. (A6)), are always much smaller than unity. Then, disregarding second or higher order contributions in  $(u - \bar{u})$  or  $(\mu - \bar{\mu})$ , Eq. (A10) becomes:

$$\frac{d\mu}{dt} = -(\bar{K}' + \bar{K}'')(\mu - \bar{\mu}) - \frac{\bar{K}'\bar{K}''}{\bar{K}' + \bar{K}''}\delta v \quad (\text{A11})$$

where we have used the steady-state condition:

$$\bar{K}'\bar{\mu} = \bar{K}''(1 - \bar{\mu}). \quad (\text{A12})$$

Substituting in Eq. (A10) the expression of  $\delta v$ , Eq. (A6), we obtain

$$\frac{d\mu}{dt} = -\left\{ \bar{K}' + \bar{K}'' + \frac{\bar{K}'\bar{K}''}{\bar{K}' + \bar{K}''} \alpha_2(1 - \alpha_2)\theta \right\} (\mu - \bar{\mu}) \quad (\text{A13})$$

and substitution of this latter expression into Eq. (A9) yields:

$$\frac{du}{dt} = -\alpha_2\theta \left\{ \bar{K}' + \bar{K}'' + \alpha_2(1 - \alpha_2)\theta \frac{\bar{K}'\bar{K}''}{\bar{K}' + \bar{K}''} \right\} (\mu - \bar{\mu}) - \left\{ \frac{1}{\tau_m} + \alpha_2^2\theta \frac{\bar{K}'\bar{K}''}{\bar{K}' + \bar{K}''} \right\} (u - \bar{u}). \quad (\text{A14})$$

Equations (A13) and (A14) are a system of two linear differential equations with constant coefficients in the two unknowns  $(u - \bar{u})$  and  $(\mu - \bar{\mu})$ . The solution of the linear differential equations (A13) and (A14) for  $u(t) - \bar{u}$  has the following form:

$$u(t) - \bar{u} = a_1 e^{-t/\tau_1} + a_2 e^{-t/\tau_2} \quad (\text{A15})$$

where  $\lambda_1 = 1/\tau_1$  and  $\lambda_2 = 1/\tau_2$  are the roots of the characteristic equation which may be written as:

$$\lambda^2 - Z_1\lambda + Z_2 = 0 \quad (\text{A16})$$

$$Z_1 = \bar{K}' + \bar{K}'' + \alpha_2\theta \frac{\bar{K}'\bar{K}''}{\bar{K}' + \bar{K}''} + \frac{1}{\tau_m} \quad (\text{A17})$$

$$Z_2 = \frac{1}{\tau_m} \left( \bar{K}' + \bar{K}'' + \alpha_2 (1 - \alpha_2) \theta \frac{\bar{K}' \bar{K}''}{\bar{K}' + \bar{K}''} \right). \quad (\text{A18})$$

According to Viëta's theorem,  $Z_1$  and  $Z_2$  may be expressed by the roots  $\lambda_1$  and  $\lambda_2$ :

$$Z_1 = \lambda_1 + \lambda_2 = \frac{1}{\tau_1} + \frac{1}{\tau_2} \quad (\text{A19})$$

$$Z_2 = \lambda_1 \cdot \lambda_2 = \frac{1}{\tau_1} \cdot \frac{1}{\tau_2}. \quad (\text{A20})$$

Furthermore, taking the time derivative of Eq. (A15) for  $t=0$ , substituting into Eq. (A14) and using the appropriate initial condition of a charge pulse experiment, i.e.:  $\mu(0) = \bar{\mu}$  and  $u(0) - \bar{u} = a_1 + \alpha_2$ , a third relation is obtained:

$$Z_3 = [a_1/\tau_1 + a_2/\tau_2](a_1 + a_2) = \alpha_2^2 \theta \frac{\bar{K}' \bar{K}''}{\bar{K}' + \bar{K}''} + \frac{1}{\tau_m}. \quad (\text{A21})$$

$\tau_m$ ,  $\bar{K}' + \bar{K}''$  and  $\theta$  can be calculated by rearrangements of Eqs. (A17), (A18), and (A21).

$$\tau_m = (Z_1 - Z_3)/Z_2 \quad (\text{A22})$$

$$2 K_{\text{eff}} = \bar{K}' + \bar{K}'' = (Z_1 - Z_3) - \left( \frac{1 - \alpha_2}{\alpha_2} \right) \left( Z_3 - \frac{Z_2}{Z_1 - Z_3} \right) \quad (\text{A23})$$

$$\alpha_2^2 \theta \bar{K}' \bar{K}'' / (\bar{K}' + \bar{K}'') = \left( Z_3 - \frac{Z_2}{Z_1 - Z_3} \right). \quad (\text{A24})$$

$\bar{v}$  is defined by Eq. (A5) and can be expressed after eliminating  $\theta$  and  $\bar{u}$  using Eqs. (A24), (A12), (A2), and (A3) - solely as a function of  $\bar{\mu}$ :

$$\bar{v} + \frac{2\{Z_3(Z_1 - Z_3) - Z_2\}(1 - \alpha_2) \sinh\{\bar{v}/2\} \cosh\{\bar{v}/2\}}{\alpha_2(Z_1 - Z_3)^2 - (1 - \alpha_2)\{Z_3(Z_1 - Z_3) - Z_2\}} = \alpha_2(\bar{u} - u_o). \quad (\text{A25})$$

For  $\alpha_2 = 1$ , the expression for  $K_{\text{eff}} = (\bar{K}' + \bar{K}'')/2$  and  $\bar{v}$  are much simplified and become:

$$K_{\text{eff}} = (Z_1 - Z_3)/2 \quad (\text{A26})$$

$$\bar{v} = \bar{u} - u_o. \quad (\text{A27})$$

## References

- Almers, W. 1978. Gating currents and charge movements in excitable membranes. *Rev. Physiol. Biochem. Pharmacol.* **82**:96
- Andersen, O.S., Feldberg, S., Nakadomari, H., Levy, S., McLaughlin, S. 1978. Electrostatic interactions among hydrophobic ions in lipid bilayer membranes. *Biophys. J.* **21**:35
- Andersen, O.S., Fuchs, M. 1975. Potential energy barriers to ion transport within lipid bilayers. Studies with tetraphenylborate. *Biophys. J.* **15**:795
- Armstrong, C.M., Bezanilla, F. 1973. Currents related to movement of the gating particles of the sodium channels. *Nature (London)* **242**:459
- Armstrong, C.M., Bezanilla, F. 1975. Currents associated with the ionic gating structures in nerve membrane. *Ann. N.Y. Acad. Sci.* **264**:265
- Benz, R., Cros, D. 1978. Influence of sterols on ion transport through lipid bilayer membranes. *Biochim. Biophys. Acta* **506**:265
- Benz, R., Fröhlich, O., Läger, P. 1977. Influence of membrane structure on the kinetics of carrier-mediated ion transport through lipid bilayers. *Biochim. Biophys. Acta* **464**:465
- Benz, R., Fröhlich, O., Läger, P., Montal, M. 1975. Electrical

capacity of black lipid films and of lipid bilayers made from monolayers. *Biochim. Biophys. Acta* **394**:323

- Benz, R., Gisin, B.F. 1978. Influence of membrane structure on ion transport through lipid bilayer membranes. *J. Membrane Biol.* **40**:293
- Benz, R., Läger, P. 1976. Kinetic analysis of carrier-mediated ion transport by the charge-pulse technique. *J. Membrane Biol.* **27**:171
- Benz, R., Läger, P. 1977. Transport kinetics of dipicrylamine through lipid bilayer membranes. Effects of membrane structure. *Biochim. Biophys. Acta* **468**:245
- Benz, R., Läger, P., Janko, K. 1976. Transport kinetics of hydrophobic ions in lipid bilayer membranes. Charge pulse relaxation studies. *Biochim. Biophys. Acta* **455**:701
- Benz, R., Nonner, W. 1980. Structure of the axolemma of frog myelinated nerve: Relaxation experiments with a lipophilic probe ion. *J. Membrane Biol.* **59**:127
- Brand, L., Gohlke, J.R. 1972. Fluorescence probes for structure. *Annu. Rev. Biochem.* **41**:808
- Bruner, L.J. 1975. The interaction of hydrophobic ions with lipid bilayer membranes. *J. Membrane Biol.* **22**:125
- Chandler, W.K., Meves, H. 1965. Voltage clamp experiments on internally perfused giant axons. *J. Physiol. (London)* **180**:788
- Conrad, M.J., Singer, S.J. 1979. Evidence for a large internal pressure in biological membranes. *Proc. Nat. Acad. Sci. USA* **76**:5202
- Conti, F. 1975. Fluorescent probes in nerve membranes. *Annu. Rev. Biophys. Bioeng.* **4**:287
- Conti, F., Fioravanti, R., Malerba, F., Wanke, E. 1974. A comparative analysis of extrinsic fluorescence in nerve membranes and lipid bilayers. *Biophys. Struct. Mechan.* **1**:27
- Conti, F., Malerba, F. 1972. Fluorescence signals in ANS-stained lipid bilayers under applied potentials. *Biophysik* **8**:326
- Dilger, J.P., McLaughlin, S., McIntosh, T.J., Simon, S.A. 1979. The dielectric constant of phospholipid bilayers and the permeability of membrane to ions. *Science* **206**:1196
- Dyson, R.D., Isenberg, I. 1971. Analysis of exponential curves by a method of moments, with special attention to sedimentation equilibrium and fluorescence decay. *Biochemistry* **10**:3233
- Feldberg, S.W., Kissel, G. 1975. Charge pulse studies of transport phenomena in bilayer membranes. I. Steady-state measurements of actin- and valinomycin-mediated transport in glycerol monooleate bilayers. *J. Membrane Biol.* **20**:269
- Frankenhaeuser, B., Hodgkin, A.L. 1956. The after-effect of impulses in the giant nerve fibres of *Loligo*. *J. Physiol. (London)* **131**:341
- Hodgkin, A.L., Huxley, A.F. 1952. A quantitative description of membrane current and its application to conduction and excitation in nerve. *J. Physiol. (London)* **117**:500
- Hubbell, W.L., McConnell, H.M. 1968. Spin-label studies of the excitable membranes of nerve and muscle. *Proc. Natl. Acad. Sci. USA* **61**:12
- Johnson, F.H., Eyring, H., Stover, B.J. 1974. The Theory of Rate Processes in Biology and Medicine. John Wiley & Sons, New York
- Jordan, P.C., Stark, G. 1979. Kinetics of transport of hydrophobic ions through lipid membranes including diffusion polarization in the aqueous phase. *Biophys. Chem.* **10**:273
- Ketterer, B., Neumcke, B., Läger, P. 1971. Transport mechanism of hydrophobic ions through lipid bilayer membranes. *J. Membrane Biol.* **5**:225
- McLaughlin, S. 1977. Electrostatic potentials at membrane-solution interfaces. In: Current Topics in Membranes and Transport. F. Bronner and A. Kleinzeller, editors. p. 71. Academic Press, New York
- McLaughlin, S., Harary, H. 1976. The hydrophobic adsorption of charged molecules to bilayer membranes: A test of the applicability of the Stern equation. *Biochemistry* **15**:1941

- Moore, J.W., Cole, K.S. 1963. Voltage clamp techniques. *Phys. Tech. Biol. Res.* **5**:263
- Neumcke, B., Läuger, P. 1969. Nonlinear electrical effects in lipid bilayer membranes. *Biophys. J.* **9**:1160
- Neumcke, B., Nonner, W., Stämpfli, R. 1978. Gating currents in excitable membranes. In: MTP International Review of Science (Biochemistry Series). Vol. 2, Series 2, p. 129. Butterworths, London
- Parsegian, A. 1969. Energy of an ion crossing a low dielectric membrane. Solutions of four relevant electrostatic problems. *Nature (London)* **221**:844
- Pickar, A.D., Benz, R. 1978. Transport of oppositely charged lipophilic probe ions in lipid bilayer membranes having various structures. *J. Membrane Biol.* **44**:353
- Rojas, E., Ehrenstein, G. 1965. Voltage clamp experiments with potassium as the only internal and external cation. *J. Cell Comp. Physiol.* **66**:71
- Sackmann, E. 1978. Dynamic molecular organization in vesicles and membranes. *Ber. Bunsenges. Phys. Chem.* **82**:891
- Seelig, A., Seelig, J. 1978. Lipid-protein interaction in reconstituted cytochrome *c*/phospholipid membranes. *Hoppe-Seyler's Z. Physiol. Chem.* **359**:1747
- Singer, S.J., Nicolson, G.L. 1972. The fluid mosaic model of the structure of cell membranes. *Science* **175**:720
- R. Benz and F. Conti: Charge Pulse Relaxation in Squid Axons
- Szabo, G. 1974. Dual mechanism for the action of cholesterol on membrane permeability. *Nature (London)* **257**:47
- Szabo, G. 1976. The influence of dipole potentials on the magnitude and the kinetics of ion transport in lipid bilayer membranes In: Extreme Environment: Mechanisms of Microbial Adaptation. M.R. Heinrich, editor. p. 321. Academic Press, New York
- Tasaki, I., Watanabe, A., Takenaka, T. 1962. Resting and action potential of intracellularly perfused squid giant axon. *Proc. Nat. Acad. Sci. USA* **48**:1177
- Webb, W.W. 1977. Lateral transport on membranes. In: Electrical Phenomena at the Biological Membrane Level. E. Roux, editor. p. 119. Elsevier, Amsterdam
- Weber, G. 1972. Uses of fluorescence in biophysics: Some recent developments. *Annu. Rev. Biophys. Bioeng.* **1**:553
- White, S.H., Petersen, D.C., Simon, S.A., Yafuso, M. 1976. Formation of planar bilayer membranes from lipid monolayers. A critique. *Biophys. J.* **16**:481
- Wulf, J., Benz, R., Pohl, W.G. 1977. Properties of bilayer membranes in the presence of dipicrylamine. A comparative study by optical absorption and electrical relaxation studies. *Biochim. Biophys. Acta* **365**:429

Received 19 June 1980; revised 27 October 1980